EUROPEAN ORGANIZATION FOR NUCLEAR RESEARCH

CERN-PPE/97-76
2 July 1997

Single and Multi-Photon Events with Missing Energy in e^+e^- Collisions at 161 GeV $< \sqrt{s} <$ 172 GeV

The L3 Collaboration

Abstract

A search for single and multi-photon events with missing energy is performed using data collected at centre-of-mass energies between 161 GeV and 172 GeV for a total of 20.9 pb^{-1} of integrated luminosity. The results obtained are used to derive the value for the $\nu\bar{\nu}\gamma(\gamma)$ cross section as well as upper limits on new physics processes.

Submitted to *Phys. Lett. B*

1 Introduction

The increase in centre-of-mass energy achieved at LEP in 1996 provides the opportunity to search for physics beyond the Standard Model. Single or double photon events with missing energy could be evidence of a variety of new physics processes: pair production of neutralinos ($\tilde{\chi}^0_1\tilde{\chi}^0_1$, $\tilde{\chi}^0_1\tilde{\chi}^0_2$, $\tilde{\chi}^0_2\tilde{\chi}^0_2$, etc.) or associated production of a neutralino and a light gravitino ($\tilde{\chi}^0_1\tilde{\mathrm{G}}$), when neutralinos follow either the decay $\tilde{\chi}^0_2 \to \tilde{\chi}^0_1\gamma$ [1] or $\tilde{\chi}^0_1 \to \tilde{\mathrm{G}}\gamma$ [2]; single or double production of excited neutrinos [3, 4] where the latter follows the decay $\nu^* \to \nu\gamma$; and finally production of an invisible resonance that is produced in association with one or more photons.

In the following we present a study of events with one or more energetic photons and missing energy. Two distinct kinematic regions are considered: high energy photons from which the cross section for the $\nu\bar{\nu}\gamma(\gamma)$ process is measured and low energy photons for which other Standard Model processes contribute significantly. Both regions are used in searching for new physics processes. Limits are derived for general models of particle production followed by radiative decay and for specific Supersymmetry models with a light gravitino.

Searches for single and multi-photon final states, as well as measurements of the $\nu\bar{\nu}\gamma(\gamma)$ cross section, have already been performed by L3 [5] and by other LEP experiments [6] at centre-of-mass energies around the Z resonance and above.

2 Data Sample

In this analysis we use the data collected by the L3 detector [7] during the high energy run of LEP in 1996 for an integrated luminosity of 10.7 pb^{-1} at $\sqrt{s} = 161.3$ GeV (hereafter called 161 GeV run), 1.0 pb^{-1} at $\sqrt{s} = 170.3$ GeV and 9.2 pb^{-1} at $\sqrt{s} = 172.3$ GeV (hereafter called 172 GeV run).

Monte Carlo events for the main background sources were simulated, namely $\mathrm{e^+e^-} \to \nu\bar{\nu}\gamma(\gamma)$, with `KORALZ` [8] and `NNGSTR` [9], $\mathrm{e^+e^-} \to \gamma\gamma(\gamma)$ with `GGG` [10], Bhabha scattering for large scattering angles with `BHAGENE` [11] and for small scattering angles with `TEEGG` [12], and finally two-photon interactions, specifically the process $\mathrm{e^+e^-} \to \mathrm{e^+e^-e^+e^-}$, with `DIAG36` [13]. The number of simulated background events corresponds to more than 50 times the integrated luminosity of the collected data for all processes except Bhabha scattering and two-photon collisions for which the number is about 10. The detector response has been fully simulated [14] for these processes.

3 Event Selection

Electrons and photons are measured in the BGO electromagnetic calorimeter (hereafter called BGO). They are required to have an energy greater than 0.9 GeV, and their energy deposition pattern in the calorimeters must be consistent with an electromagnetic shower. Electrons are defined as electromagnetic clusters matched with a charged track reconstructed in the central tracking chamber. Identified conversion electrons coming from photons that have interacted with the beam pipe or with the silicon microvertex detector are also treated as photon candidates. We define the barrel region to subtend the polar angle range $43^\circ < \theta < 137^\circ$ with respect to the beam axis and the end-cap region to subtend the range $14^\circ < \theta < 37^\circ$ or $143^\circ < \theta < 166^\circ$. Bhabha events and $\mathrm{e^+e^-} \to \gamma\gamma$ events that are fully contained in the calorimeter are used to

check the particle identification as well as the energy resolution, which is found to be 1.8% for beam-energy electrons and photons in both the barrel and the end-caps.

3.1 High Energy Photons

The selection of high energy photon candidates aims at identifying single and multi-photon events while rejecting radiative Bhabha events and bremsstrahlung photons from out-of-time cosmic rays. The following event requirements are imposed:

- there must be at least one photon with energy greater than 10 GeV in the barrel or end-cap region;
- the total detected energy not assigned to the identified photons must be smaller than 10 GeV;
- there must be no charged tracks or there must be exactly two charged tracks consistent with a photon conversion.

To suppress background from events with particles that are not photons, we require the energy in the hadron calorimeter to be smaller than 10 GeV. To ensure good containment of particles, precise energy measurement and reliable particle identification we require the energy in the EGAP (electromagnetic calorimeter between BGO barrel and end-caps) to be smaller than 10 GeV in the 161 GeV run and smaller than 7 GeV in the 172 GeV run, the energy in the active lead rings to be smaller than 2 GeV and the energy in the luminosity monitor to be smaller than 3 GeV. To reject cosmic ray background, we require events with no identified muon tracks and require that the most energetic BGO cluster not be aligned with signals in the muon detector. There must also be at least one scintillator time measurement within 30° in azimuthal angle that falls within 5 ns of the beam crossing time. In addition, there must be no more than one BGO cluster not associated with an identified photon.

To reject backgrounds from radiative Bhabha events and the process $e^+e^- \to \gamma\gamma(\gamma)$, we also require:

- the total transverse momentum ($P_\perp$) of photons must be greater than 6 GeV;
- the opening angle between the two jets constructed from all calorimetric clusters in each hemisphere must be smaller than 177.6°, both in three dimensions and as projected in the plane transverse to the beam axis.

When a second photon with energy greater than 5 GeV is present, then the following alternative selection is applied to the two most energetic BGO clusters in order to reject the above backgrounds:

- their opening angle must be less than 177.6° in the plane transverse to the beam;
- their total transverse momentum must be greater than 3 GeV;
- the recoil mass calculated from $\sqrt{s + M^2_{\gamma\gamma} - 2\sqrt{s}E_{\gamma\gamma}}$ must have a real solution.

After applying this selection, for the 161 GeV run, we observe in the data 35 events in the barrel, with one or more photons, and 22 in the end-caps to be compared with a Monte Carlo prediction of 26.7 and 27.2 events, respectively. For the 172 GeV run we observe in the data 25

Observed two photon events		#1	#2	#3
First photon	Energy	36.2 GeV	37.9 GeV	45.0 GeV
	Polar angle	45.8°	29.8°	54.4°
	Azimuthal angle	114.0°	189.6°	151.8°
Second photon	Energy	19.8 GeV	12.9 GeV	6.1 GeV
	Polar angle	146.7°	56.7°	55.0°
	Azimuthal angle	253.8°	310.0°	260.1°
Transverse momentum of the event		19.1 GeV	16.2 GeV	35.4 GeV
Two photon mass		51.9 GeV	26.7 GeV	21.9 GeV
Two photon recoil mass		103.2 GeV	101.7 GeV	112.1 GeV

Table 1: Characteristics of the observed two photon events, at $\sqrt{s} = 161$ GeV (#1 and #2) and at $\sqrt{s} = 172$ GeV (#3), with recoil mass larger than 100 GeV.

events in the barrel and 24 in the end-caps to be compared with a Monte Carlo prediction of 21.7 and 24.5 events. The selected sample is nearly pure $\nu\bar{\nu}\gamma(\gamma)$, with only 0.3 events expected from radiative Bhabha events and the process $e^+e^- \to \gamma\gamma(\gamma)$, for both the 161 and 172 GeV runs. The observed rates of two photon events and of photon conversions agree well with the Monte Carlo simulation. The cosmic ray background in the final event sample is estimated to be 0.05 ± 0.05 events in the barrel region and 1.16 ± 0.8 events in the end-caps region, based on studies of out-of-time events.

The selection and trigger efficiency for $\nu\bar{\nu}\gamma(\gamma)$ events contained in the fiducial volume defined above and satisfying the kinematic requirements ($E_\gamma > 10$ GeV, $P_\perp > 6$ GeV) is estimated to be $(81.4 \pm 0.6)\%$ for the barrel and $(79.9 \pm 0.6)\%$ for the end-caps. Figure 1 shows the two photon invariant mass and recoil mass distributions for the $\nu\bar{\nu}\gamma\gamma(\gamma)$ Monte Carlo and for the data, selected with a minimum energy cut on the second photon of 1 GeV. We observe 6 events in the data compared to the Monte Carlo prediction of 7.8 events (2.4 events with a recoil mass larger than 100 GeV). The main characteristics of the three events with recoil mass larger than 100 GeV are summarized in Table 1. Figure 2 shows the recoil mass distribution for single and multi-photon events.

3.2 Low Energy Photons

This selection extends the search for photonic final states to the low energy range. The search covers only the barrel region where a single photon trigger is implemented with a threshold at around 900 MeV [15]. To prevent overlap with the previous selection, a maximum energy of 10 GeV has been set. In this selection the total luminosity used is 10.0 pb^{-1} for the 161 GeV run and 9.7 pb^{-1} for the 172 GeV run. We apply the following selection requirements:

- the energy in the hadron calorimeter must be less than 3 GeV;
- there must be no significant energy deposition in the forward detectors;
- neither a track in the central tracking chamber nor a muon track is present;
- there must be exactly one energy deposition between 1.3 GeV and 10 GeV in the fiducial region of $45° < \theta < 135°$ satisfying electromagnetic shape criteria;

- there must be no other BGO clusters in the barrel or end-caps, with energy greater than 200 MeV;
- the transverse momentum of the photon must be greater than 1.3 GeV.

Specific problems at low energy are the increase of the background due to cosmic ray events and to low angle radiative Bhabha scattering, with the forward scattered electron below the minimum tagging angle of the detector. To remove cosmic ray events we impose stringent requirements on the transverse shape of the photon shower. With the increase in beam energy, for radiative Bhabha events where only the photon is detected, the third order process becomes insufficient to describe data at low transverse momentum. We simulate the process $e^+e^- \to e^+e^-\gamma(\gamma)$ with the `TEEGG` [12] Monte Carlo, where we have included the fourth order contribution.

After applying the selection requirements we expect, according to the Monte Carlo, 28.2 and 24.5 events and we observe in the data 27 and 28 events for the 161 GeV run and the 172 GeV run, respectively. In particular, we expect 11.4 events from the $e^+e^- \to \nu\bar{\nu}\gamma(\gamma)$ process, 41.3 events from radiative Bhabha events and a negligible contribution from the $e^+e^- \to \gamma\gamma(\gamma)$ process. The efficiencies of this selection for $\nu\bar{\nu}\gamma(\gamma)$ events in the fiducial volume defined above and satisfying the kinematic requirements (1.3 GeV $< E_\gamma <$ 10 GeV and $P_\perp >$ 1.3 GeV) are 74.4% and 73.9% for the 161 GeV run and 172 GeV run, respectively. The trigger efficiency is included in these values. The cosmic ray background in this sample is estimated to be 2.1 ± 0.4 events.

In Figure 3 we show the energy spectrum of the photon for the combined samples at 161 GeV and 172 GeV. It should be noticed that below 4 GeV the background from radiative Bhabha events becomes substantial.

4 Systematic Checks

Radiative Bhabha scattering events where one electron enters the barrel region while other particles escape at low polar angles (so-called single electron events) constitute a control sample similar to the single photon sample. For this reason a single electron sample from the data is used to perform systematic checks.

The overall trigger efficiency, for the high energy photon selection, is the combination of the single photon trigger (barrel only) and of the BGO cluster trigger [15]. Since the minimum photon energy required in this selection is well above the threshold of these two triggers, the main sources of the inefficiency ($\approx$1%) are found to be inactive trigger and read out channels. For low energy photons the single photon trigger is the most important because the BGO cluster trigger has a threshold of roughly 6 GeV. The trigger efficiency has been evaluated using a trigger simulation and also directly from the data, using the single electron sample, taking advantage of redundant triggers.

The single electron sample has also been used to perform checks on the simulation of electromagnetic showers in the calorimeter and on energy resolution in the $0 - 5$ GeV range, and to estimate the efficiency loss due to cosmic ray veto requirements. Using randomly triggered beam-gate events we estimate the additional inefficiency ($\approx$2%) due to noise sources not simulated in the Monte Carlo, such as that induced by beam halo in the forward detectors. Further checks have been done to compare the Monte Carlo prediction of `KORALZ` [8] with that of `NNGSTR` [9] for the $e^+e^- \to \nu\bar{\nu}\gamma$ process. We observe good agreement in predicted energy distributions and cross sections, which are consistent within $3 - 4\%$.

5 Results

5.1 $\nu\bar{\nu}\gamma(\gamma)$ Cross Section Measurement

To measure the cross section of the $\nu\bar{\nu}\gamma(\gamma)$ process we restrict the analysis to photon energies above 10 GeV. Below this value the signal to background ratio is much lower. For the 161 GeV run we observe 57 events, and we expect 54.7 events including 0.8 cosmic ray events. For the 172 GeV run we observe 49 events with 46.6 events expected, including 0.4 cosmic ray events. Since the background contamination, for the selected energy range, is very small (between 1% and 2%) the uncertainty on the background efficiency is unimportant. The error on the measured luminosity is less than 1%. A total systematic uncertainty on the efficiency due to photon identification cuts has been estimated to be 1.6%.

The efficiency for the $e^+e^- \to \nu\bar{\nu}\gamma(\gamma)$ process for events contained in the fiducial volume defined above and satisfying the kinematic requirements ($E_\gamma > 10$ GeV, $P_\perp > 6$ GeV) is $80.5 \pm 0.6\ (stat) \pm 1.4\ (syst)\%$ at $\sqrt{s} = 161$ GeV and $80.7 \pm 0.6 \pm 1.4\%$ at $\sqrt{s} = 172$ GeV. The measured cross section at $\sqrt{s} = 161$ GeV is:

$$\sigma_{\nu\bar{\nu}\gamma(\gamma)} = 6.75 \pm 0.91\ (stat) \pm 0.18\ (syst)\ \text{ pb}$$

and at $\sqrt{s} = 172$ GeV is

$$\sigma_{\nu\bar{\nu}\gamma(\gamma)} = 6.12 \pm 0.89\ (stat) \pm 0.14\ (syst)\ \text{ pb.}$$

These measurements are converted into the total cross section for $\nu\bar{\nu}(\gamma)$ production to obtain (78.4 ± 10.9) pb at $\sqrt{s} = 161$ GeV and (73.5 ± 10.9) pb at $\sqrt{s} = 172$ GeV. The Standard Model predictions are 72.1 pb and 66.7 pb, respectively. The large statistical errors on these cross sections and the significant contribution expected from $t-$channel production through W exchange preclude deriving a useful measurement of the number of neutrino families.

5.2 Limits on New Physics

A variety of new processes can give rise to events with single or multiple photons with missing energy. Both the high energy selection and the low energy selection are used to set limits. For the single photon signature, we consider the simple hypothesis of isotropic photon production in the laboratory frame. For the two photon signature, we also consider specific interpretations in Supersymmetry models with a light gravitino.

We first consider the general process $e^+e^- \to XY \to \gamma XX$, with $M_Y > M_X$. To derive cross section limits for specific M_X and M_Y pairings, we apply the requirement (additional to those described in sections 3.1 and 3.2) that the most energetic photon in the event have an energy kinematically consistent with M_Y and M_X. Since we assume isotropic photon production, we restrict the photon candidates to the barrel region. Figure 4 shows the resulting 95% C.L. upper limits on the cross sections for the process $e^+e^- \to XY \to \gamma XX$. Figure 5-a shows the limit on the luminosity weighted average cross section when the two samples at 161 GeV and at 172 GeV are combined. Figure 5-b shows these limits when $M_X \simeq 0$ is assumed.

We also consider the general process $e^+e^- \to YY \to \gamma\gamma XX$ with $M_X \simeq 0$, using the specific process $e^+e^- \to \tilde{\chi}_1^0\tilde{\chi}_1^0 \to \tilde{G}\tilde{G}\gamma\gamma$ for estimating detection efficiencies. To search for this process, we require two identified photons in the detector. To suppress the background from $\nu\bar{\nu}\gamma\gamma(\gamma)$, two additional requirements are imposed:

- the difference between the recoil mass of the two photons and the Z boson mass must be greater than 6.5 GeV;
- the energy of both photons must be greater than the kinematically allowed minimum value for $M_{\tilde{\chi}_1^0}$.

The SPYTHIA Monte Carlo generator [16] has been used to estimate the signal efficiency. Monte Carlo events for the process $e^+e^- \to \tilde{\chi}_1^0\tilde{\chi}_1^0 \to \tilde{G}\tilde{G}\gamma\gamma$ have been produced for several different values of the $\tilde{\chi}_1^0$ mass and for a gravitino light enough to ensure a decay of the $\tilde{\chi}_1^0$ close to the production point ($c\tau_{\tilde{\chi}_1^0} \sim 2 \cdot 10^{-3}[M_{\tilde{\chi}_1^0}/100\ \mathrm{GeV}]^{-5}[M_{\tilde{G}}/1\ \mathrm{eV}]^2$ cm). The signal efficiency, the background expectation and the number of candidate events in the data versus the mass of the lightest neutralino are shown in Figure 6-a. The derived cross section limits are plotted in Figure 6-b versus the neutralino mass.

5.3 Interpretations in Specific SUSY Models

After combining the two centre-of-mass energies, we calculate the upper limit on the number of events expected from a neutralino signal (Figure 7). The theoretical prediction for a no scale supergravity model (LNZ [17]) and three extreme cases for the neutralino composition, which determines its coupling to the photon and to the Z, are plotted in the same figure. From this, we derive the following lower limits on the mass of the lightest neutralino within these special scenarios at 95% confidence level:

LNZ	$M_{\tilde{\chi}_1^0} > 66.1$ GeV;
Photino	$M_{\tilde{\chi}_1^0} > 68.6$ GeV;
Bino	$M_{\tilde{\chi}_1^0} > 64.8$ GeV;
Higgsino	$M_{\tilde{\chi}_1^0} > 75.3$ GeV.

One can also interpret these results in terms of limits on the parameters of the minimal supersymmetric standard model (MSSM [18]), still assuming a light gravitino scenario. We then translate the cross section limits on $\tilde{\chi}_1^0\tilde{\chi}_1^0$ production into exclusion regions in the $M_2 - \mu$ plane (Figure 8) with M_2 being the SU(2) gaugino mass parameter and μ the SUSY Higgs-mixing mass in the MSSM parameter space. The exclusion is given for two different values of $\tan\beta$, the ratio of the Higgs vacuum expectation values, and for two values of m_0, the common scalar mass. The excluded region decreases for increasing values of m_0.

6 Acknowledgements

We wish to congratulate the CERN accelerator divisions for the successful upgrade of the LEP machine and to express our gratitude for its good performance. We acknowledge with appreciation the effort of all engineers, technicians and support staff who have participated in the construction and maintenance of this experiment. We thank G. Kane for fruitful discussions.

References

[1] P. Fayet, Phys. Lett. B 117 (1982) 460;
H.E. Haber and D. Wyler, Nucl. Phys. **B 323** (1989) 267;
S. Ambrosanio and B. Mele, Phys. Rev. **D53** (1996) 2541;
S. Ambrosanio *et al.*, Phys. Rev. Lett. **76** (1996) 3498.

[2] J. Ellis and J.S. Hagelin, Phys. Lett. **B 122** (1983) 303;
J. Ellis *et al.*, Phys. Lett. **B 147** (1984) 99;
P. Fayet , Phys. Lett. B 175 (1986) 471;
S. Dimopoulos *et al.*, Phys. Rev. Lett. **76** (1996) 3494;
D.R. Stump *et al.*, Phys. Rev. **D54** (1996) 1936.

[3] F. Boudjema *et al.*, in "Z Physics at LEP 1", CERN Report CERN 89-08, eds. G. Altarelli, R. Kleiss and C. Verzegnassi (CERN, Geneva, 1989) Vol. 2, p. 188 and references therein.

[4] K. Hagiwara *et al.*, Z. Phys. **C 29** (1985) 115.

[5] L3 Collab., B. Adeva *et al.*, Phys. Lett. **B 275** (1992) 209;
L3 Collab., O. Adriani *et al.*, Phys. Lett. **B 292** (1992) 463;
L3 Collab., O. Adriani *et al.*, Phys. Lett. **B 297** (1992) 469;
L3 Collab., M. Acciarri *et al.*, Phys. Lett. **B 346** (1995) 190;
L3 Collab., M. Acciarri *et al.*, Phys. Lett. **B 370** (1996) 195.

[6] ALEPH Collab., D. Buskulic *et al.*, Phys. Lett. **B 313** (1993) 520;
ALEPH Collab., D. Buskulic *et al.*, Phys. Lett. **B 384** (1996) 333;
DELPHI Collab., P. Abreu *et al.*, Phys. Lett. **B 380** (1996) 471;
DELPHI Collab., P. Abreu *et al.*, Z. Phys. **C 74** (1997) 577;
OPAL Collab., R. Akers *et al.*, Z. Phys. **C 65** (1995) 47;
OPAL Collab., K. Ackerstaff *et al.*, Phys. Lett. **B 391** (1997) 210.

[7] The L3 Collaboration, B. Adeva *et al.*, Nucl. Instr. and Meth. **A 289** (1990) 35;
M. Chemarin *et al.*, Nucl. Instr. and Meth. **A 349** (1994) 345;
M. Acciarri *et al.*, Nucl. Instr. and Meth. **A 351** (1994) 300;
G. Basti *et al.*, Nucl. Instr. and Meth. **A 374** (1996) 293;
I.C. Brock *et al.*, Nucl. Instr. and Meth. **A 381** (1996) 236;
A. Adam *et al.*, Nucl. Instr. and Meth. **A 383** (1996) 342.

[8] The KORALZ version 4.01 is used.
S. Jadach, B.F.L. Ward and Z. Wąs, Comp. Phys. Comm. **79** (1994) 503.

[9] R. Miquel *et al.*, Z. Phys. **C 48** (1990) 309;
F.A. Berends *et al.*, Nucl. Phys. **B 301** (1988) 583.

[10] F.A. Berends and R. Kleiss, Nucl. Phys. **B 186** (1981) 22.

[11] J.H. Field, Phys. Lett. **B 323** (1994) 432;
J.H. Field and T. Riemann, Comp. Phys. Comm. **94** (1996) 53.

[12] The TEEGG version 7.1 is used.
D. Karlen, Nucl. Phys. **B 289** (1987) 23.

[13] F.A. Berends, P.H. Daverfeldt and R. Kleiss, Nucl. Phys. **B 253** (1985) 441.

[14] The L3 detector simulation is based on GEANT Version 3.15.
See R. Brun *et al.*, "GEANT 3", CERN DD/EE/84-1 (Revised), September 1987.
The GHEISHA program (H. Fesefeldt, RWTH Aachen Report PITHA 85/02 (1985)) is used to simulate hadronic interactions.

[15] R. Bizzarri *et al.*, Nucl. Inst. Meth. **A 317** (1992) 463.

[16] S. Mrenna, "`SPYTHIA`, A Supersymmetric Extension of `PYTHIA 5.7`",
Comp. Phys. Comm. **101** (1997) 232.

[17] J.L. Lopez and D.V. Nanopoulos, Phys. Rev. **D 55** (1997) 4450.

[18] Y.A. Golfand and E.P. Likhtman, Sov. Phys. JETP **13** (1971) 323;
D.V. Volkhov and V.P. Akulov, Phys. Lett. **B 46** (1973) 109;
J. Wess and B. Zumino, Nucl. Phys. **B 70** (1974) 39;
P. Fayet and S. Ferrara, Phys. Rep. **C 32** (1977) 249;
A. Salam and J. Strathdee, Fortschr. Phys. **26** (1978) 57.

The L3 Collaboration:

M.Acciarri,[29] O.Adriani,[18] M.Aguilar-Benitez,[28] S.Ahlen,[12] J.Alcaraz,[28] G.Alemanni,[24] J.Allaby,[19] A.Aloisio,[31] G.Alverson,[13] M.G.Alviggi,[31] G.Ambrosi,[21] H.Anderhub,[51] V.P.Andreev,[7,40] T.Angelescu,[14] F.Anselmo,[10] A.Arefiev,[30] T.Azemoon,[3] T.Aziz,[11] P.Bagnaia,[39] L.Baksay,[46] S.Banerjee,[11] Sw.Banerjee,[11] K.Banicz,[48] A.Barczyk,[51,49] R.Barillère,[19] L.Barone,[39] P.Bartalini,[36] A.Baschirotto,[29] M.Basile,[10] R.Battiston,[36] A.Bay,[24] F.Becattini,[18] U.Becker,[17] F.Behner,[51] J.Berdugo,[28] P.Berges,[17] B.Bertucci,[36] B.L.Betev,[51] S.Bhattacharya,[11] M.Biasini,[19] A.Biland,[51] G.M.Bilei,[36] J.J.Blaising,[4] S.C.Blyth,[37] G.J.Bobbink,[2] R.Bock,[1] A.Böhm,[1] L.Boldizsar,[15] B.Borgia,[39] D.Bourilkov,[51] M.Bourquin,[21] S.Braccini,[21] J.G.Branson,[42] V.Brigljevic,[51] I.C.Brock,[37] A.Buffini,[18] A.Buijs,[47] J.D.Burger,[17] W.J.Burger,[21] J.Busenitz,[46] A.Button,[3] X.D.Cai,[17] M.Campanelli,[51] M.Capell,[17] G.Cara Romeo,[10] G.Carlino,[31] A.M.Cartacci,[18] J.Casaus,[28] G.Castellini,[18] F.Cavallari,[39] N.Cavallo,[31] C.Cecchi,[21] M.Cerrada,[28] F.Cesaroni,[25] M.Chamizo,[28] Y.H.Chang,[53] U.K.Chaturvedi,[20] S.V.Chekanov,[33] M.Chemarin,[27] A.Chen,[53] G.Chen,[8] G.M.Chen,[8] H.F.Chen,[22] H.S.Chen,[8] X.Chereau,[4] G.Chiefari,[31] C.Y.Chien,[5] L.Cifarelli,[41] F.Cindolo,[10] C.Civinini,[18] I.Clare,[17] R.Clare,[17] H.O.Cohn,[34] G.Coignet,[4] A.P.Colijn,[2] N.Colino,[28] V.Commichau,[1] S.Costantini,[9] F.Cotorobai,[14] B.de la Cruz,[28] A.Csilling,[15] T.S.Dai,[17] R.D'Alessandro,[18] R.de Asmundis,[31] A.Degré,[4] K.Deiters,[49] D.della Volpe,[31] P.Denes,[38] F.DeNotaristefani,[39] D.DiBitonto,[46] M.Diemoz,[39] D.van Dierendonck,[2] F.Di Lodovico,[51] C.Dionisi,[39] M.Dittmar,[51] A.Dominguez,[42] A.Doria,[31] M.T.Dova,[20,♯] D.Duchesneau,[4] P.Duinker,[2] I.Duran,[43] S.Dutta,[11] S.Easo,[36] Yu.Efremenko,[34] H.El Mamouni,[27] A.Engler,[37] F.J.Eppling,[17] F.C.Erné,[2] J.P.Ernenwein,[27] P.Extermann,[21] M.Fabre,[49] R.Faccini,[39] S.Falciano,[39] A.Favara,[18] J.Fay,[27] O.Fedin,[40] M.Felcini,[51] B.Fenyi,[46] T.Ferguson,[37] F.Ferroni,[39] H.Fesefeldt,[1] E.Fiandrini,[36] J.H.Field,[21] F.Filthaut,[37] P.H.Fisher,[17] I.Fisk,[42] G.Forconi,[17] L.Fredj,[21] K.Freudenreich,[51] C.Furetta,[29] Yu.Galaktionov,[30,17] S.N.Ganguli,[11] P.Garcia-Abia,[50] S.S.Gau,[13] S.Gentile,[39] N.Gheordanescu,[14] S.Giagu,[39] S.Goldfarb,[24] J.Goldstein,[12] Z.F.Gong,[22] A.Gougas,[5] G.Gratta,[35] M.W.Gruenewald,[9] V.K.Gupta,[38] A.Gurtu,[11] L.J.Gutay,[48] B.Hartmann,[1] A.Hasan,[32] D.Hatzifotiadou,[10] T.Hebbeker,[9] A.Hervé,[19] W.C.van Hoek,[33] H.Hofer,[51] S.J.Hong,[45] H.Hoorani,[37] S.R.Hou,[53] G.Hu,[5] V.Innocente,[19] K.Jenkes,[1] B.N.Jin,[8] L.W.Jones,[3] P.de Jong,[19] I.Josa-Mutuberria,[28] A.Kasser,[24] R.A.Khan,[20] D.Kamrad,[50] Yu.Kamyshkov,[34] J.S.Kapustinsky,[26] Y.Karyotakis,[4] M.Kaur,[20,◇] M.N.Kienzle-Focacci,[21] D.Kim,[39] D.H.Kim,[45] J.K.Kim,[45] S.C.Kim,[45] Y.G.Kim,[45] W.W.Kinnison,[26] A.Kirkby,[35] D.Kirkby,[35] J.Kirkby,[19] D.Kiss,[15] W.Kittel,[33] A.Klimentov,[17,30] A.C.König,[33] A.Kopp,[50] I.Korolko,[30] V.Koutsenko,[17,30] R.W.Kraemer,[37] W.Krenz,[1] A.Kunin,[17,30] P.Ladron de Guevara,[28] I.Laktineh,[27] G.Landi,[18] C.Lapoint,[17] K.Lassila-Perini,[51] P.Laurikainen,[23] M.Lebeau,[19] A.Lebedev,[17] P.Lebrun,[27] P.Lecomte,[51] P.Lecoq,[19] P.Le Coultre,[51] J.M.Le Goff,[19] R.Leiste,[50] E.Leonardi,[39] P.Levtchenko,[40] C.Li,[22] C.H.Lin,[53] W.T.Lin,[53] F.L.Linde,[2,19] L.Lista,[31] Z.A.Liu,[8] W.Lohmann,[50] E.Longo,[39] W.Lu,[35] Y.S.Lu,[8] K.Lübelsmeyer,[1] C.Luci,[39] D.Luckey,[17] L.Luminari,[39] W.Lustermann,[49] W.G.Ma,[22] M.Maity,[11] G.Majumder,[11] L.Malgeri,[39] A.Malinin,[30] C.Maña,[28] D.Mangeol,[33] S.Mangla,[11] P.Marchesini,[51] A.Marin,[12] J.P.Martin,[27] F.Marzano,[39] G.G.G.Massaro,[2] D.McNally,[19] R.R.McNeil,[7] S.Mele,[31] L.Merola,[31] M.Meschini,[18] W.J.Metzger,[33] M.von der Mey,[1] Y.Mi,[24] A.Mihul,[14] A.J.W.van Mil,[33] G.Mirabelli,[39] J.Mnich,[19] P.Molnar,[9] B.Monteleoni,[18] R.Moore,[3] S.Morganti,[39] T.Moulik,[11] R.Mount,[35] S.Müller,[1] F.Muheim,[21] A.J.M.Muijs,[2] S.Nahn,[17] M.Napolitano,[31] F.Nessi-Tedaldi,[51] H.Newman,[35] T.Niessen,[1] A.Nippe,[1] A.Nisati,[39] H.Nowak,[50] Y.D.Oh,[45] H.Opitz,[1] G.Organtini,[39] R.Ostonen,[23] C.Palomares,[28] D.Pandoulas,[1] S.Paoletti,[39] P.Paolucci,[31] H.K.Park,[37] I.H.Park,[45] G.Pascale,[39] G.Passaleva,[18] S.Patricelli,[31] T.Paul,[13] M.Pauluzzi,[36] C.Paus,[1] F.Pauss,[51] D.Peach,[19] Y.J.Pei,[1] S.Pensotti,[29] D.Perret-Gallix,[4] B.Petersen,[33] S.Petrak,[9] A.Pevsner,[5] D.Piccolo,[31] M.Pieri,[18] J.C.Pinto,[37] P.A.Piroué,[38] E.Pistolesi,[29] V.Plyaskin,[30] M.Pohl,[51] V.Pojidaev,[30,18] H.Postema,[17] N.Produit,[21] D.Prokofiev,[40] G.Rahal-Callot,[51] N.Raja,[11] P.G.Rancoita,[29] M.Rattaggi,[29] G.Raven,[42] P.Razis,[32] K.Read,[34] D.Ren,[51] M.Rescigno,[39] S.Reucroft,[13] T.van Rhee,[47] S.Riemann,[50] K.Riles,[3] A.Robohm,[51] J.Rodin,[17] B.P.Roe,[3] L.Romero,[28] S.Rosier-Lees,[4] Ph.Rosselet,[24] W.van Rossum,[47] S.Roth,[1] J.A.Rubio,[19] D.Ruschmeier,[9] H.Rykaczewski,[51] J.Salicio,[19] E.Sanchez,[28] M.P.Sanders,[33] M.E.Sarakinos,[23] S.Sarkar,[11] M.Sassowsky,[1] C.Schäfer,[1] V.Schegelsky,[40] S.Schmidt-Kaerst,[1] D.Schmitz,[1] P.Schmitz,[1] N.Scholz,[51] H.Schopper,[52] D.J.Schotanus,[33] J.Schwenke,[1] G.Schwering,[1] C.Sciacca,[31] D.Sciarrino,[21] L.Servoli,[36] S.Shevchenko,[35] N.Shivarov,[44] V.Shoutko,[30] J.Shukla,[26] E.Shumilov,[30] A.Shvorob,[35] T.Siedenburg,[1] D.Son,[45] A.Sopczak,[50] B.Smith,[17] P.Spillantini,[18] M.Steuer,[17] D.P.Stickland,[38] A.Stone,[7] H.Stone,[38] B.Stoyanov,[44] A.Straessner,[1] K.Strauch,[16] K.Sudhakar,[11] G.Sultanov,[20] L.Z.Sun,[22] G.F.Susinno,[21] H.Suter,[51] J.D.Swain,[20] X.W.Tang,[8] L.Tauscher,[6] L.Taylor,[13] Samuel C.C.Ting,[17] S.M.Ting,[17] M.Tonutti,[1] S.C.Tonwar,[11] J.Tóth,[15] C.Tully,[38] H.Tuchscherer,[46] K.L.Tung,[8] Y.Uchida,[17] J.Ulbricht,[51] U.Uwer,[19] E.Valente,[39] R.T.Van de Walle,[33] G.Vesztergombi,[15] I.Vetlitsky,[30] G.Viertel,[51] M.Vivargent,[4] R.Völkert,[50] H.Vogel,[37] H.Vogt,[50] I.Vorobiev,[30] A.A.Vorobyov,[40] A.Vorvolakos,[32] M.Wadhwa,[6] W.Wallraff,[1] J.C.Wang,[17] X.L.Wang,[22] Z.M.Wang,[22] A.Weber,[1] F.Wittgenstein,[19] S.X.Wu,[20] S.Wynhoff,[1] J.Xu,[12] Z.Z.Xu,[22] B.Z.Yang,[22] C.G.Yang,[8] X.Y.Yao,[8] J.B.Ye,[22] S.C.Yeh,[53] J.M.You,[37] An.Zalite,[40] Yu.Zalite,[40] P.Zemp,[51] Y.Zeng,[1] Z.Zhang,[8] Z.P.Zhang,[22] B.Zhou,[12] G.Y.Zhu,[8] R.Y.Zhu,[35] A.Zichichi,[10,19,20] F.Ziegler.[50]

1 I. Physikalisches Institut, RWTH, D-52056 Aachen, FRG§
III. Physikalisches Institut, RWTH, D-52056 Aachen, FRG§
2 National Institute for High Energy Physics, NIKHEF, and University of Amsterdam, NL-1009 DB Amsterdam, The Netherlands
3 University of Michigan, Ann Arbor, MI 48109, USA
4 Laboratoire d'Annecy-le-Vieux de Physique des Particules, LAPP,IN2P3-CNRS, BP 110, F-74941 Annecy-le-Vieux CEDEX, France
5 Johns Hopkins University, Baltimore, MD 21218, USA
6 Institute of Physics, University of Basel, CH-4056 Basel, Switzerland
7 Louisiana State University, Baton Rouge, LA 70803, USA
8 Institute of High Energy Physics, IHEP, 100039 Beijing, China△
9 Humboldt University, D-10099 Berlin, FRG§
10 University of Bologna and INFN-Sezione di Bologna, I-40126 Bologna, Italy
11 Tata Institute of Fundamental Research, Bombay 400 005, India
12 Boston University, Boston, MA 02215, USA
13 Northeastern University, Boston, MA 02115, USA
14 Institute of Atomic Physics and University of Bucharest, R-76900 Bucharest, Romania
15 Central Research Institute for Physics of the Hungarian Academy of Sciences, H-1525 Budapest 114, Hungary‡
16 Harvard University, Cambridge, MA 02139, USA
17 Massachusetts Institute of Technology, Cambridge, MA 02139, USA
18 INFN Sezione di Firenze and University of Florence, I-50125 Florence, Italy
19 European Laboratory for Particle Physics, CERN, CH-1211 Geneva 23, Switzerland
20 World Laboratory, FBLJA Project, CH-1211 Geneva 23, Switzerland
21 University of Geneva, CH-1211 Geneva 4, Switzerland
22 Chinese University of Science and Technology, USTC, Hefei, Anhui 230 029, China△
23 SEFT, Research Institute for High Energy Physics, P.O. Box 9, SF-00014 Helsinki, Finland
24 University of Lausanne, CH-1015 Lausanne, Switzerland
25 INFN-Sezione di Lecce and Universitá Degli Studi di Lecce, I-73100 Lecce, Italy
26 Los Alamos National Laboratory, Los Alamos, NM 87544, USA
27 Institut de Physique Nucléaire de Lyon, IN2P3-CNRS,Université Claude Bernard, F-69622 Villeurbanne, France
28 Centro de Investigaciones Energeticas, Medioambientales y Tecnologicas, CIEMAT, E-28040 Madrid, Spain♭
29 INFN-Sezione di Milano, I-20133 Milan, Italy
30 Institute of Theoretical and Experimental Physics, ITEP, Moscow, Russia
31 INFN-Sezione di Napoli and University of Naples, I-80125 Naples, Italy
32 Department of Natural Sciences, University of Cyprus, Nicosia, Cyprus
33 University of Nijmegen and NIKHEF, NL-6525 ED Nijmegen, The Netherlands
34 Oak Ridge National Laboratory, Oak Ridge, TN 37831, USA
35 California Institute of Technology, Pasadena, CA 91125, USA
36 INFN-Sezione di Perugia and Universitá Degli Studi di Perugia, I-06100 Perugia, Italy
37 Carnegie Mellon University, Pittsburgh, PA 15213, USA
38 Princeton University, Princeton, NJ 08544, USA
39 INFN-Sezione di Roma and University of Rome, "La Sapienza", I-00185 Rome, Italy
40 Nuclear Physics Institute, St. Petersburg, Russia
41 University and INFN, Salerno, I-84100 Salerno, Italy
42 University of California, San Diego, CA 92093, USA
43 Dept. de Fisica de Particulas Elementales, Univ. de Santiago, E-15706 Santiago de Compostela, Spain
44 Bulgarian Academy of Sciences, Central Lab. of Mechatronics and Instrumentation, BU-1113 Sofia, Bulgaria
45 Center for High Energy Physics, Korea Adv. Inst. of Sciences and Technology, 305-701 Taejon, Republic of Korea
46 University of Alabama, Tuscaloosa, AL 35486, USA
47 Utrecht University and NIKHEF, NL-3584 CB Utrecht, The Netherlands
48 Purdue University, West Lafayette, IN 47907, USA
49 Paul Scherrer Institut, PSI, CH-5232 Villigen, Switzerland
50 DESY-Institut für Hochenergiephysik, D-15738 Zeuthen, FRG
51 Eidgenössische Technische Hochschule, ETH Zürich, CH-8093 Zürich, Switzerland
52 University of Hamburg, D-22761 Hamburg, FRG
53 High Energy Physics Group, Taiwan, China

§ Supported by the German Bundesministerium für Bildung, Wissenschaft, Forschung und Technologie
‡ Supported by the Hungarian OTKA fund under contract numbers T14459 and T24011.
♭ Supported also by the Comisión Interministerial de Ciencia y Tecnología
♯ Also supported by CONICET and Universidad Nacional de La Plata, CC 67, 1900 La Plata, Argentina
♢ Also supported by Panjab University, Chandigarh-160014, India
△ Supported by the National Natural Science Foundation of China.

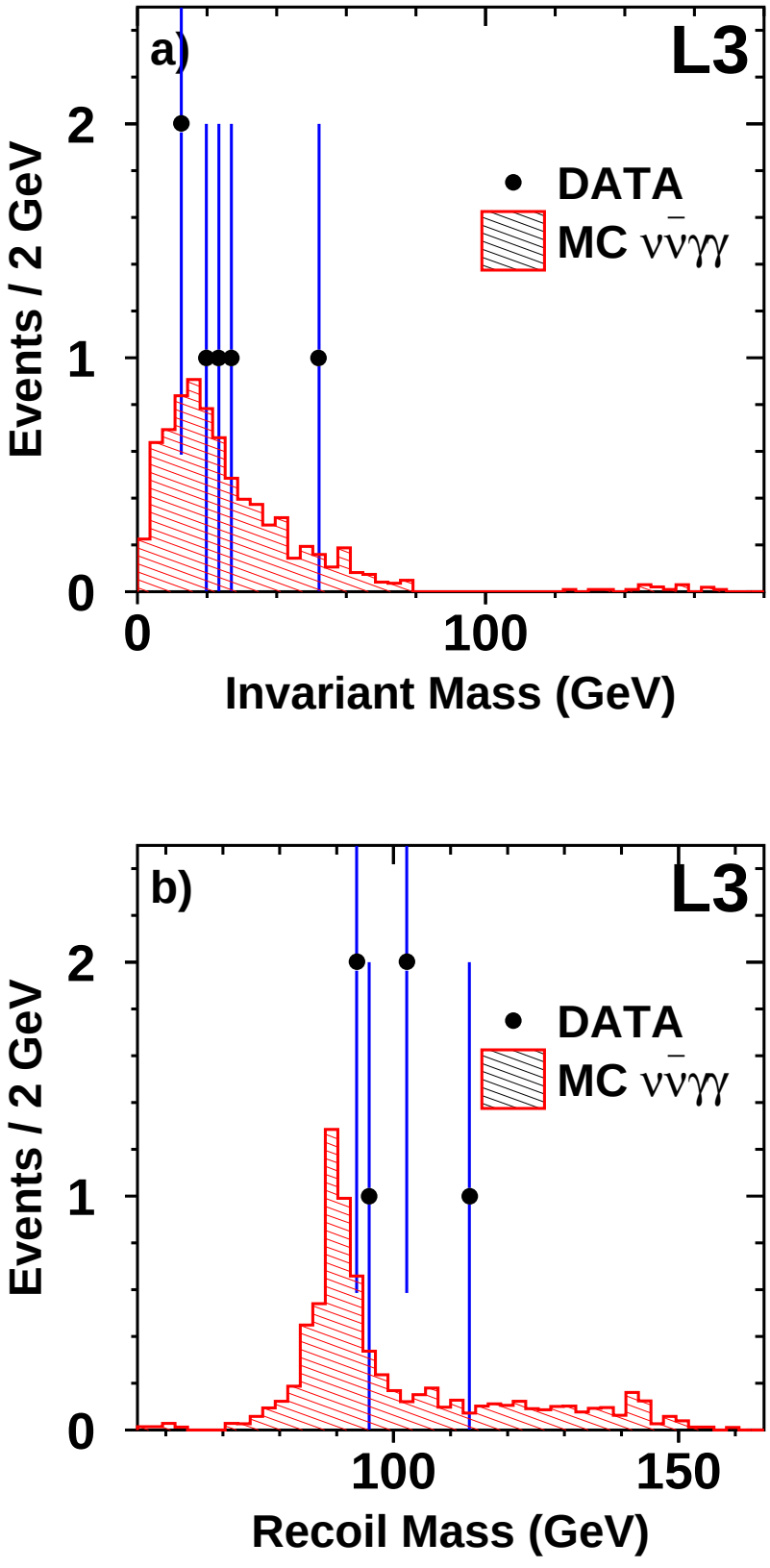

Figure 1: a) two photon invariant mass distribution for the $\nu\bar{\nu}\gamma\gamma(\gamma)$ sample. b) two photon recoil mass for the same sample.

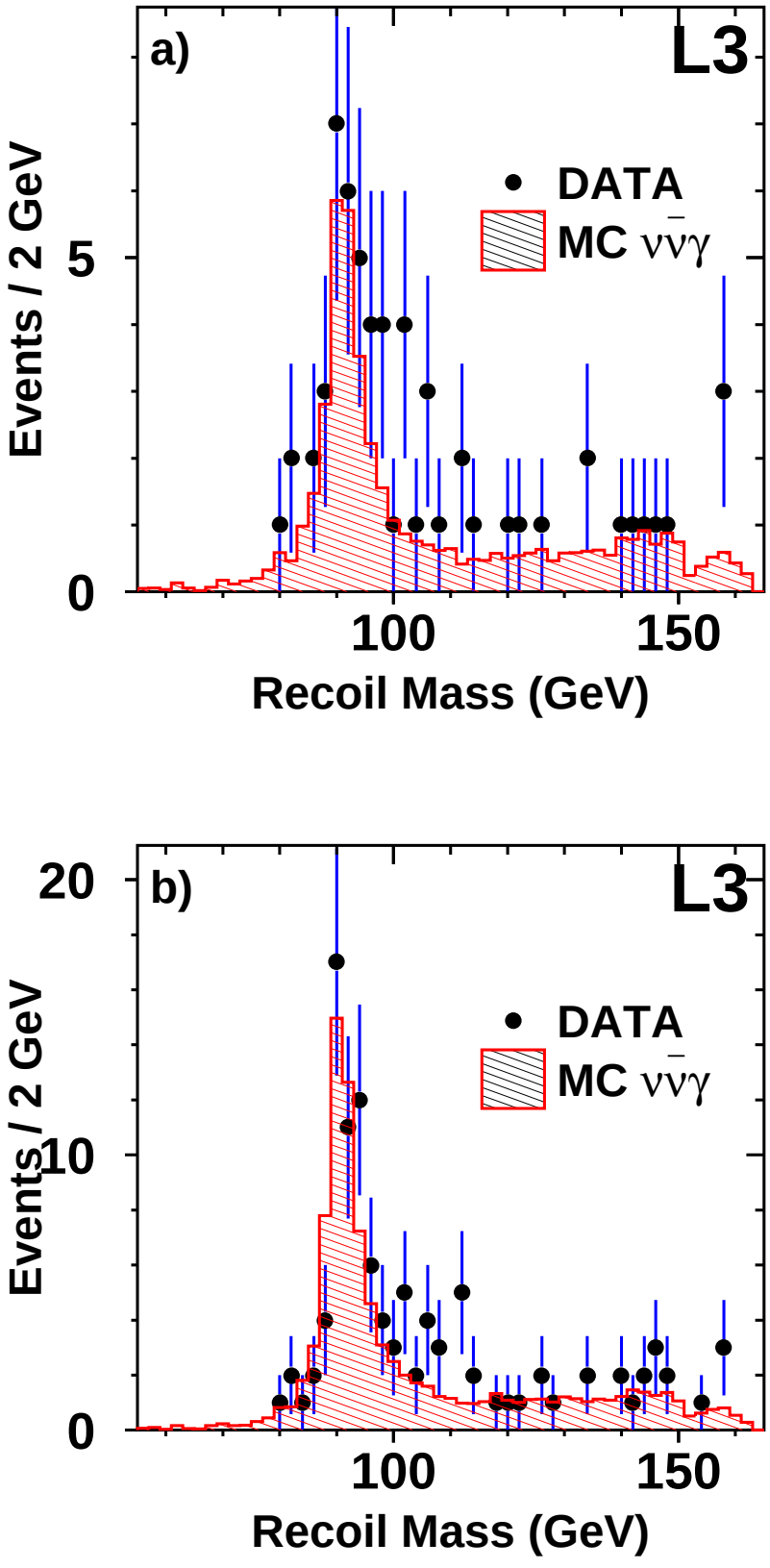

Figure 2: a) recoil mass distribution for single and multi-photon events in the barrel region, for the selected $\nu\bar{\nu}\gamma(\gamma)$ sample. b) the same distribution when the end-caps are also included.

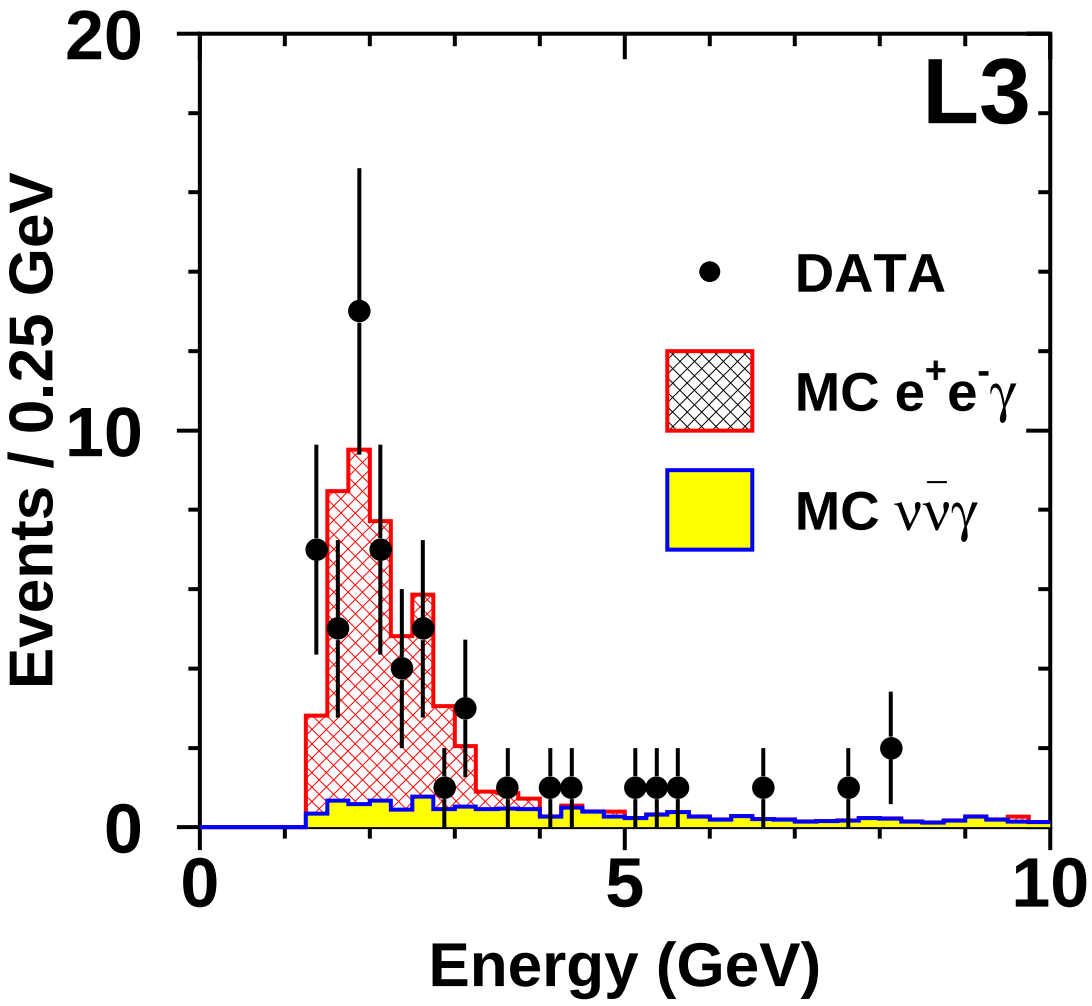

Figure 3: Energy spectrum of the selected low energy photons in the fiducial region $45^\circ < \theta < 135^\circ$.

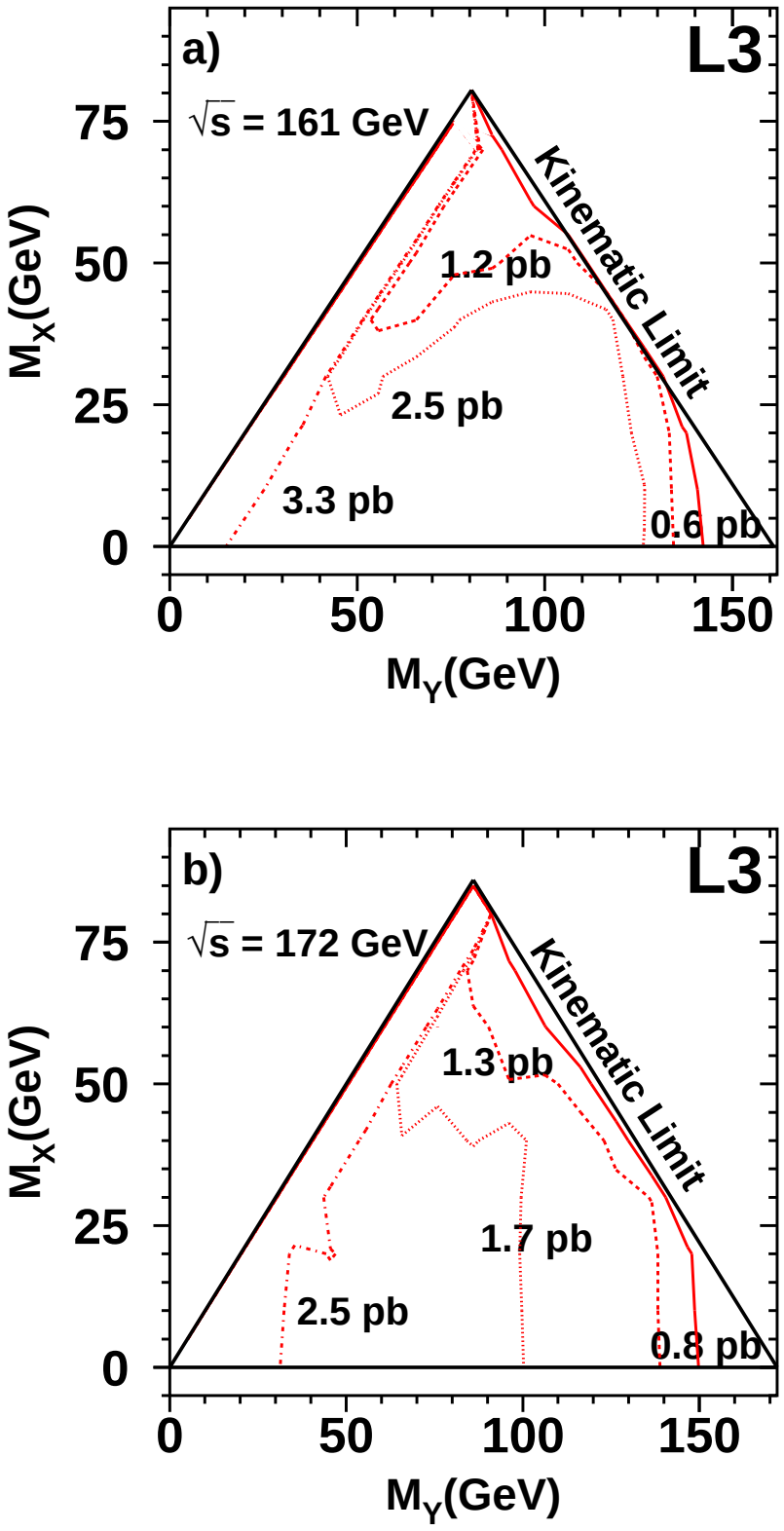

Figure 4: Upper limits at 95% C.L. on the production cross section for the process $e^+e^- \to XY \to \gamma XX$, a) at $\sqrt{s} = 161$ GeV and b) at $\sqrt{s} = 172$ GeV.

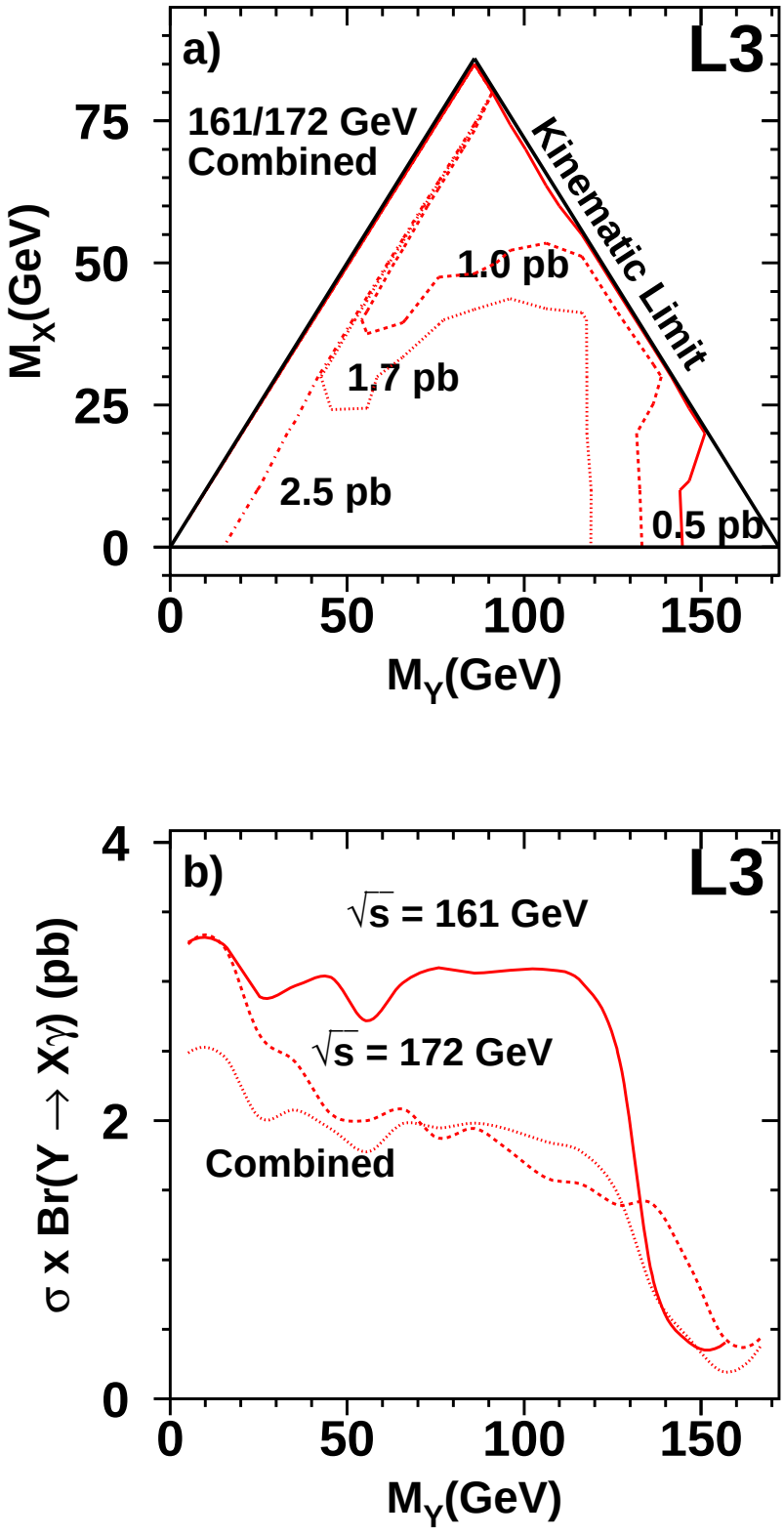

Figure 5: a) upper limit at 95% C.L. on the luminosity weighted average production cross section for the process $e^+e^- \to XY \to \gamma XX$ when the two samples at 161 GeV and at 172 GeV are combined. b) upper limits at 95% C.L. on the production cross section when $M_X \simeq 0$ is assumed.

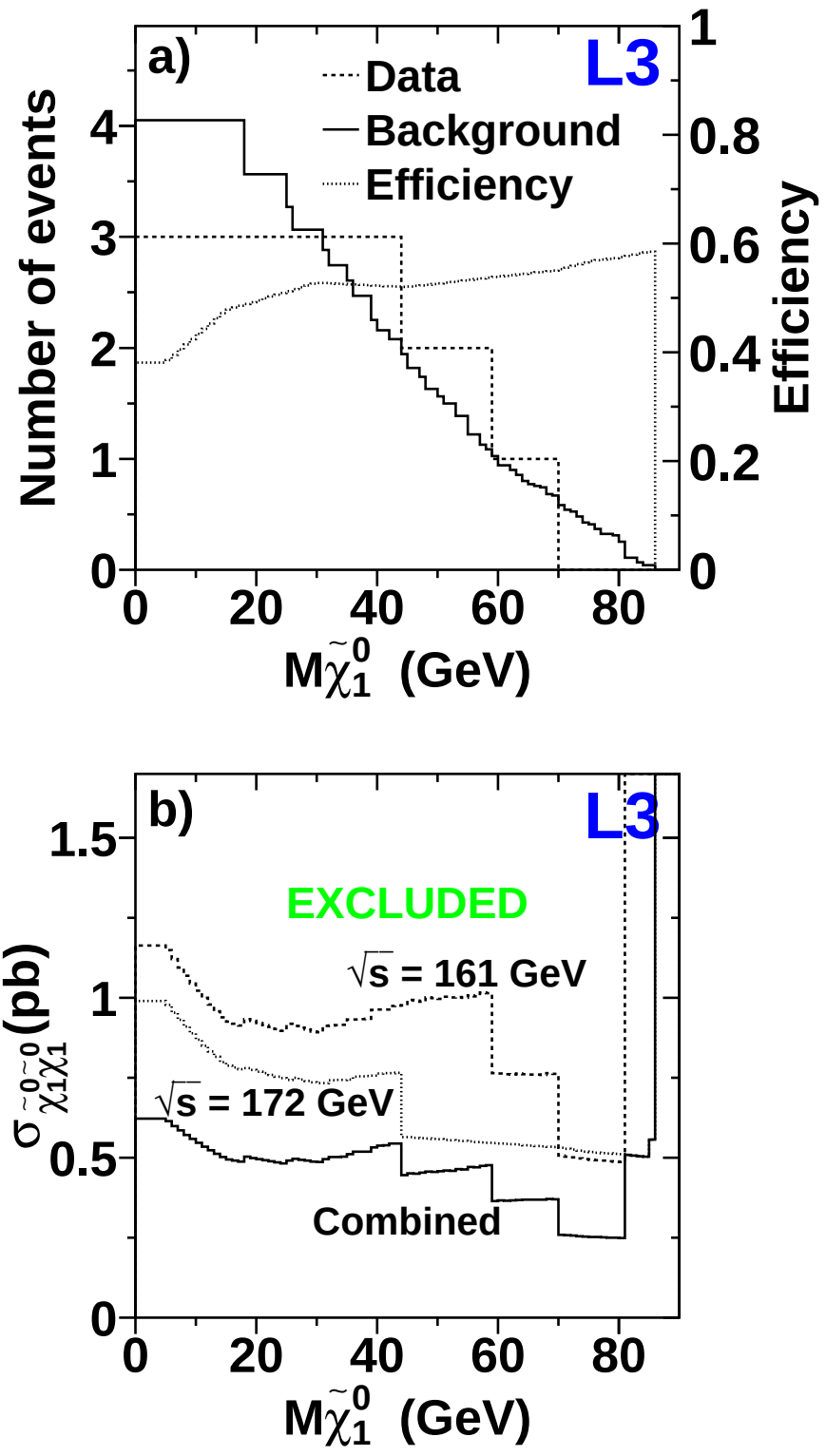

Figure 6: a) number of expected background events, number of candidate events and signal efficiency versus the mass of the $\tilde{\chi}_1^0$. b) cross section upper limits at 95% C.L. for $e^+e^- \to \tilde{\chi}_1^0\tilde{\chi}_1^0 \to \tilde{G}\tilde{G}\gamma\gamma$ at 161 GeV and 172 GeV centre-of-mass energies versus $M_{\tilde{\chi}_1^0}$. The limit obtained with the combined data sample is also shown.

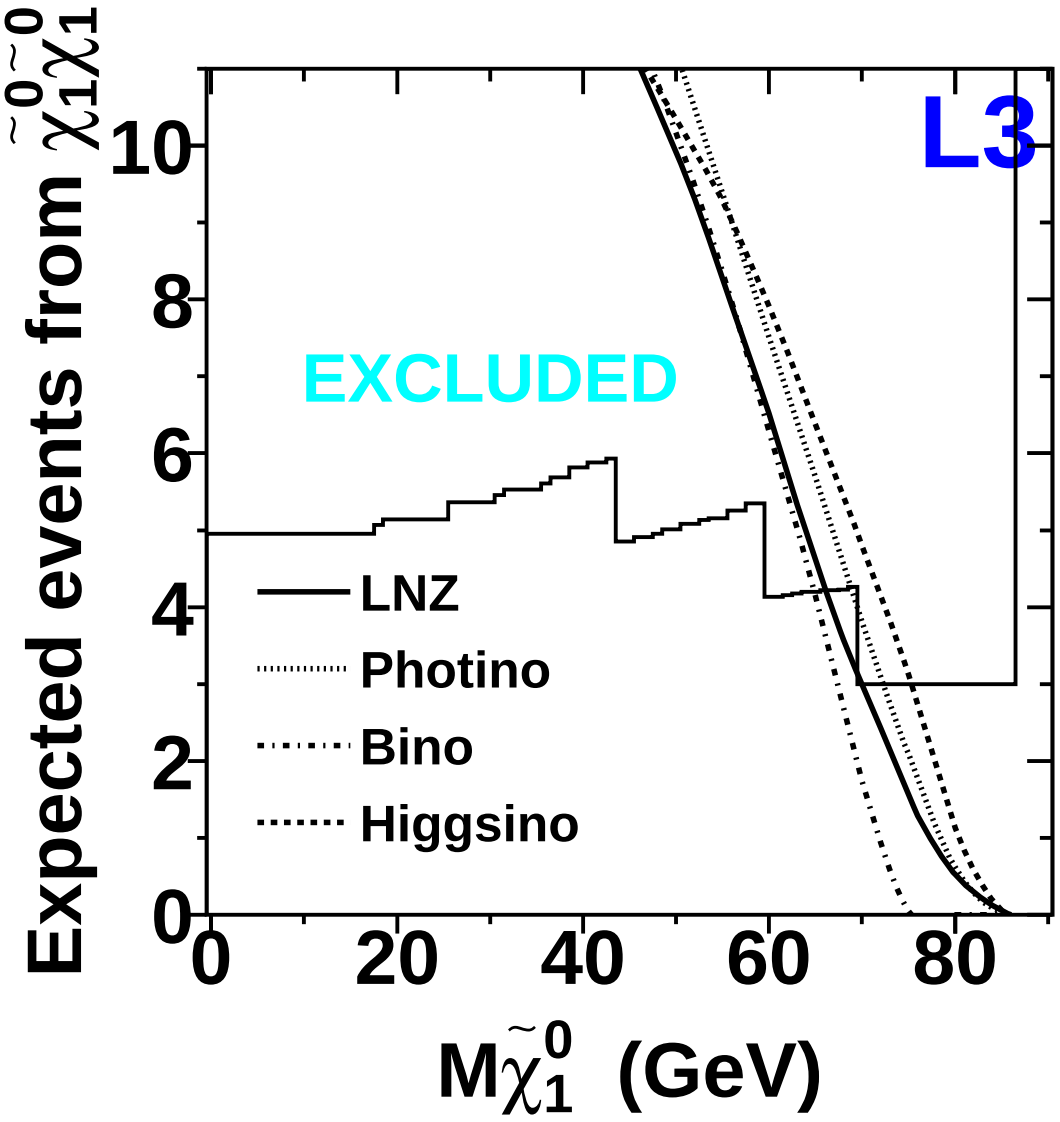

Figure 7: 95% C.L. upper limit on the number of events expected for two photon events for 161 GeV run and 172 GeV run added. LNZ gives the prediction for a no scale supergravity model. The cross section is taken from [17]. The cross sections for the pure photino, bino and higgsino were computed using SPYTHIA. For the photino and bino case a selectron mass of 90 GeV was taken. The cross section for a pure zino is too small to give a limit and hence is not plotted.

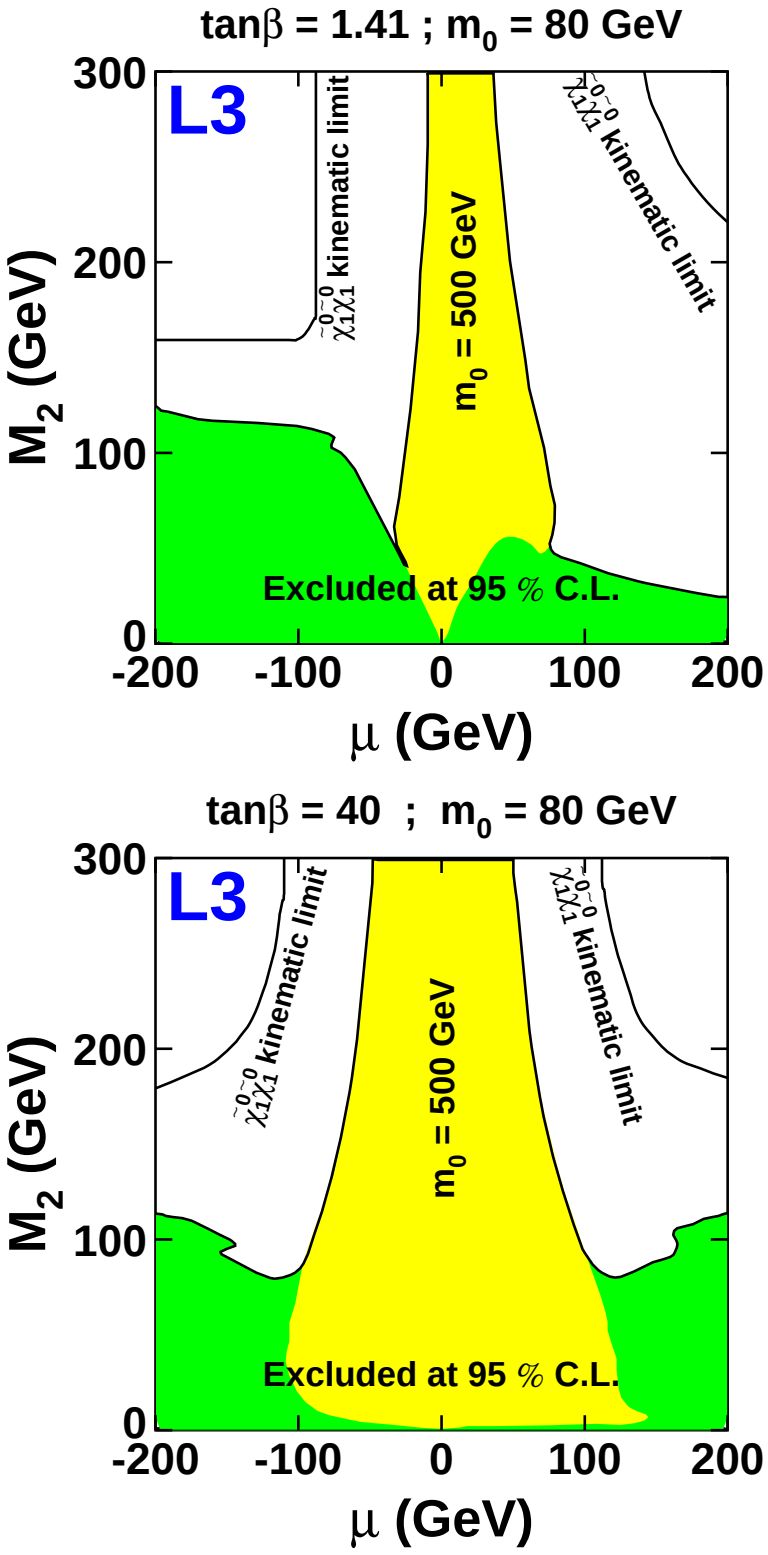

Figure 8: Excluded region in the $M_2 - \mu$ plane for different values of $\tan\beta$ and m_0. The kinematic limit for $\tilde{\chi}_1^0\tilde{\chi}_1^0$ production is also plotted. For $m_0 = 80$ GeV both the dark shaded and the light shaded regions are excluded, while for $m_0 = 500$ GeV only the light shaded region is excluded.